Appl. Phys. A 47, 399–407(1988)

Applied Physics A Solids and Surfaces

Study of Recombination Reactions of Particles Adsorbed on Fractal and Multifractal Substrata*

E. V. Albano** and H. O. Mártin

Instituto de Investigaciones Fisicoquímicas Teóricas y Aplicadas (INIFTA), Facultad de Ciencias Exactas. Universidad Nacional de La Plata, Sucursal 4, Casilla de Correo 16, La Plata, Argentina
Departamento de Física, Facultad de Ciencias Exactas, Universidad Nacional de La Plata, Casilla de Correo 67, (1900) La Plata, Argentina

Received 29 April 1988/Accepted 9 June 1988

Abstract. Recombination reactions of adsorbed particles on fractal and multifractal media are discussed within the framework of the random walk arguments. Theoretical results, which predict anomalous reaction order $X>2$ in the low coverage regime, are checked by means of Monte Carlo simulations on two-dimensional structures and good agreement is found. Thermal desorption experiments on rough surfaces are simulated by studying temperature programmed reactions on fractal percolating clusters. For this case the simulations give $X \cong 2.5$, i.e. the fractal reaction order is greater than the classical one ($X=2$). The influence of chemisorbed impurities (poison) on the recombination reaction is also studied and the reaction order is found to increase beyond $X=2.5$ when increasing the concentration of poison. Isothermal (recombination) desorption from energetically heterogeneous surfaces is simulated on two-dimensional substrata with multifractal distributions of activation energy of diffusion. For this case X (with $X>2$) depends on the energetic heterogeneity of the substrata ($X=2$ for an homogeneous substratum). The obtained results point out that the fractal chemical kinetic behaviour is not only restricted to the low concentration regime, but it also covers the medium coverage regime, i.e. it holds for a monolayer surface coverage $\theta \leqq 0.4$ in fractal percolating clusters.

PACS: 82.65J, 66.30

The concept of fractal is a useful tool to describe many physical systems [1]. Most fractal structures known to date have become familiar to us through theoretical works and computer simulations images, in spite of the fact that the nature offers a rich source of *macroscopic* fractal objects. Within the last group, the following examples could be mentioned: landscapes, turbulence, electrical discharges, clouds, biological structures [1–3], etc. On the other hand, examples from the theory are: infinite percolation clusters [6, 7], diffusion limited aggregates, polymer models, clustering of clusters, etc. (see for example the reviews [3–6]). Recently, Pfeifer, Avnir, and Farin [7–12 and references cited therein] have extensively demonstrated that the surface of most solids at the molecular scale may also be regarded as *microscopic* fractal structures which can be treated with the same conceptual simplicity as for macroscopic examples [9]. The fractal dimension is a quantitative measurement of the surface irregularity and it is useful for the comparison of surface physical properties, for example the fractal dimension of Pd clusters changes from $D=2.15$ to $D=2.33$ due to a methanation reaction [13]. Recently, the methods

* Financially supported by the Consejo Nacional de Investigaciones Científicas y Técnicas (CONICET) de la República Argentina

** Present address: Institut für Physik, Universität, Postfach 3980, D-6500 Mainz 1, Fed. Rep. Germany

employed in order to determine the fractal dimension of surfaces, both theoretically and experimentally, have been extensively discussed [12, 14, 15]. Examples of fractal structures also relevant in the field of surface science are coke particles [16], discontinuous thin metal films [17, 18], gold colloids [19], and electrochemical aggregates [20].

There is another aspect of fractal structures, dealing with the diffusion of random walkers, which is of great importance in surface science, that is the so-called fractal chemical kinetics [21–24 and references cited therein]. In fact, random walkers on fractals structures exhibit anomalous long time diffusion [25, 26] which indicates that the low concentration regime of chemical reactions occurring on such media is also anomalous. The understanding of this effect, which causes the reaction rate to decrease with respect to the expected one for homogeneous surfaces, would be of great importance, for instance, in certain reactions occurring in fractal catalysists. In fact, a typical catalyst is composed by fractal clusters of metal (Pt, Rh, Pd or their alloys forming particles with diameters between 10 and 100 Å [13]) supported on fractal substrates (γ/Al_2O_3, zeolites, etc. [9, 11]).

The aim of this work is to investigate a recombination reaction on fractal structures. Explicitly by using the Monte Carlo simulation, the following cases have been studied: (a) a temperature programmed recombination reaction on two-dimensional percolation clusters, as an example of thermal desorption from geometrically heterogeneous (fractal) surfaces; (b) the influence, on the above reaction process, of impurities blocking active sites of the percolating clusters; and (c) a recombination reaction at constant temperature on two-dimensional multifractal substrata as an example of isothermal reaction on energetically heterogeneous surface.

1. The Substrata

1.1. Percolating Clusters in Two-Dimensions

The percolation problem is a well established field of physics. Its detailed description lies beyond the aim of the present work, therefore the reader is directed to the reviews of [4–6] for further details. Let us briefly discuss the percolation model in the two-dimensional square lattice. It is assumed that each site of the lattice of size LxL, can be either occupied by only one particle with probability (p) or empty with probability ($1-p$). A cluster is defined as a group of particles connected by nearest neighbour distances. On an $L\times L$ square lattice a percolating cluster is a cluster which has either its length or its width (or both) equal to L. It is well known that in the thermodynamic limit ($L\to\infty$) there is a critical probability (p_c) such that for $p_c<p$ there is no percolating cluster and for $p=p_c$ one infinite percolating cluster abruptly appears for the first time. The best available value of p_c for site percolation in the square lattice is $p_c=0.5927\pm0.0001$ [27].

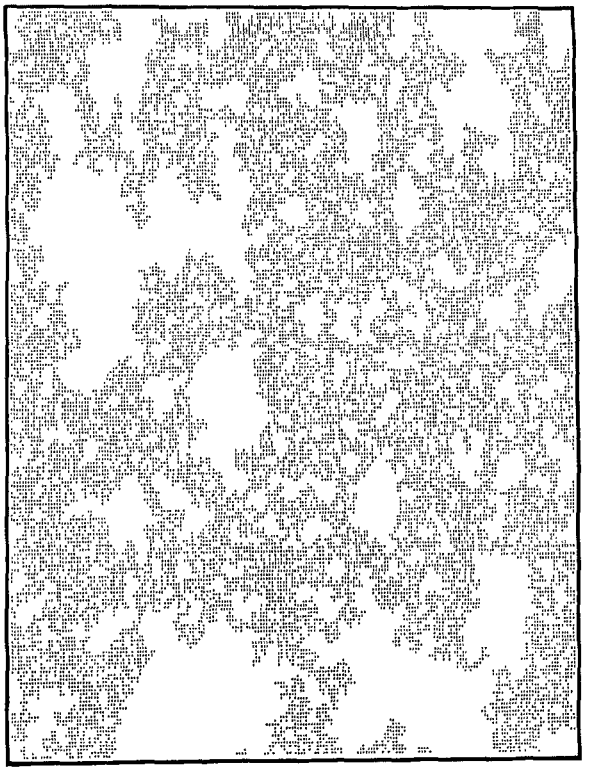

Fig. 1. An example of a percolating cluster on a square lattice of size $L=201$ at $p=0.593$. The cluster has $\sim$15,000 particles and periodic boundary conditions are imposed. The enlargement of the vertical axis is due to the computer printer

Figure 1 shows a typic percolating cluster on a square lattice of size $L=201$ at p_c. Note the heterogeneous structure due to the presence of dangling ends and holes on all scales.

Recently, a renewed interest in percolation models has arisen due to the fractal properties of the percolation cluster at p_c. In fact, theoretical results, obtained from both scaling arguments and Monte Carlo simulation, show that the fractal dimension of the percolation cluster is $D=91/48$, in agreement with measurements on very thin films [17, 28, 29]. Due to the geometrical heterogeneities characteristic of percolation clusters (see Fig. 1), these structures can be regarded as suitable substrata for the simulation of temperature programmed reactions on rough surfaces of isoenergetic sites.

1.2. Multifractal Lattice in Two Dimensions

Multifractality [1] is related to the decomposition of a fractal object into many fractal sets, each of them with

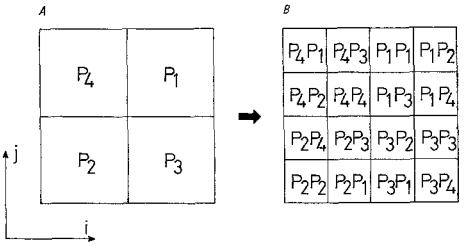

Fig. 2A, B. Scheme showing the construction sequence of a multifractal lattice. (A) First generation; (B) second generation

its own fractal dimension [30]. Let us direct our attention to the square lattice with a multifractal distribution of site probability for random walkers, as recently proposed by Meakin [31]. This kind of multifractal lattice, which will be employed in the present work, is constructed as follows (see Fig. 2). Four normalized probabilities P_m ($m=1,\ldots,4$), which characterize the multifractal, are selected. In the first step, these probabilities are randomly assigned to the four quadrants of the square lattice (Fig. 2a). In the second step, each quadrant is divided into four smaller quadrants and the probabilities previously associated with these quadrants are multiplied by P_1, P_2, P_3, and P_4 in random order (Fig. 2b). By starting with a lattice of size $2^n \times 2^n$ the process is continued for n generations. Therefore, a certain probability or measure $\mu(i,j)$ of the form:

$$\mu(i,j)=P_1^{l_1}P_2^{l_2}P_3^{l_3}P_4^{l_4} \tag{1}$$

with $l_1+l_2+l_3+l_4=n$ is associated to each lattice site of coordinates (i,j). The number of sites n_s with a measure given by (1) is $n_s=n!/l_1!l_2!l_3!l_4!$. Additional degeneracy could appear depending on each particular choice of the probabilities P_m. In the limit $n\to\infty$ the above procedure defines a multifractal measure on the two-dimensional space [32, 33]. Multifractals have also been used to describe turbulence [34].

Recently, Meakin [31] has studied the properties of random walkers on these lattices by assuming that the jumping probability P_{AB} from an A site with coordinates (i,j) into a nearest neighbour site B with coordinates (i',j') is given by:

$$P_{AB}=\begin{cases}\mu(i',j')/\mu(i,j) & \text{if} \quad \mu(i',j')<\mu(i,j)\\ 1, & \text{otherwise.}\end{cases} \tag{2}$$

We recall that the measures may be written as

$$\mu(i,j)=\exp[-E(i,j)/kT], \tag{3}$$

where $E(i,j)$ can be thought as the effective activation energy of diffusion of the random walker at the site with coordinates (i,j), which differs from the true one by an additive constant, T is the temperature and k is the Boltzmann constant. In this sense the surface has energetic heterogeneities characterized by a multifractal distribution of site probabilities. Therefore, (2) corresponds to the standard method of Metropolis et al. [35]. In the following we will work with multifractals characterized by a single parameter R ($0<R\leqq 1$) such that the probabilities P_m are given by:

$$P_m=CR^{m-1}, \quad m=1,\ldots,4, \tag{4}$$

where

$$C=\left[\sum_{i=1}^{4} R^{i-1}\right]^{-1} \tag{5}$$

is the normalization constant.

Let us denote by f_E the fraction of lattice sites with a given effective activation energy for diffusion after n generations. That is $f_E=N_E/2^n\times 2^n$, where N_E is the number of sites with dimensionless energy E/kT. In Fig. 3, the distribution of energetic heterogeneities f_E is plotted as a function of E/kT. These curves are symmetric with respect to their maximum value. Also the curve width and the position of the maximum in the energy axis depend on both the number generations and the parameter R (the former dependence is not shown in Fig. 3). Let us note that selecting $P_1=P_2=1/2(1+R)$ and $P_3=P_4=R/2(1+R)$, after n generations one has a binomial distribution of μ which, in the limit $n\to\infty$, becomes well-known Gaussian distribution frequently assumed for the description of energetically heterogeneous surfaces. Nevertheless, it should be mentioned that in the usual Gaussian distribution, the sites of different energy are randomly distributed on the surface (i.e. this kind of distribution does not define a multifractal measure). On the other hand, the spatial distribution of measures plays a fundamental role in the physical properties of the multifractal, determining that such structures are characterized by an uncountable set of generalized dimensions (for more details see for example references [32, 33]).

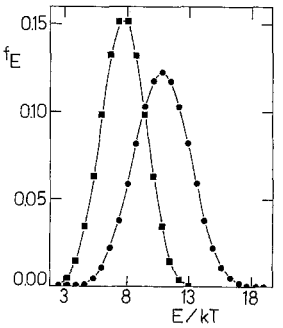

Fig. 3. Plot of the fraction f_E of lattice sites with a dimensionless activation energy of diffusion E/kT for multifractals characterized by $R=0.5$. ■ $n=5$ and ● $n=8$ generations, respectively. The lines have been drawn as a guide to the eye

We consider that the lattices just described, with a strong heterogeneous probability distribution are appropriated for the simulation of recombination reactions on energetically heterogeneous surfaces at constant temperature, which implies the conservation of the measure (3) throughout the reaction. The energetic heterogeneities could be due, for example, to the presence of surface defects at an atomic level, the chemisorption of impurities acting either as promotors or inhibitors, etc.

2. Theory of Diffusion-Limited Recombination Reactions on Fractal and Multifractal Media

2.1. Reaction on Fractal and Multifractal Substrata at Constant Temperature

In order to obtain the reaction rate equation which holds for fractal media, let us discuss the relevant behaviour of a random walker. For the long time regime, the mean number of distinct sites (S_N) visited for a random walker after N jumps, (i.e. the so called exploration space) is given by [26]:

$$S_N \sim N^f, \quad N \to \infty, \tag{6}$$

where f is the random walk exponent. $f=1$ for euclidean d-dimensional substrata with $d \geqq 2$ (classical diffusion) while $f<1$ gives anomalous diffusion. For fractals, $f=\tilde{d}/2$, for $\tilde{d}<2$, where $\tilde{d}$ is the spectral dimension related to the density of states for scalar harmonic excitations of the fractal [25, 26].

For fractal media one has that N is strictly proportional to the time t. On the other hand, for multifractal media, one can assume that this proportionality is valid in the average. Nevertheless, this assumption is not trivial at all, since the jumping probability depends strongly on the spatial region of substrata.

Considering the diffusion limited recombination of A particles

$$A_s + A_s \to \text{products}_g, \tag{7}$$

where the subscripts s and g refer to the surface and gas phase, respectively, the macroscopic reaction constant K can be related to the microscopic quantity S_N through the site visitation efficiency [23]

$$K \sim \varepsilon \equiv dS_N/dt. \tag{8}$$

Therefore, the rate equation which describes the recombination of A particles (7) becomes [23, 26, 36]

$$-d\theta/dt = C_0' \theta^X, \quad \theta \to 0, \tag{9}$$

where C_0' is a constant and the reaction order X is now given by

$$X = \begin{cases} 1+1/f & \text{if } f<1 \\ 2 & \text{if } f=1. \end{cases} \tag{10}$$

Therefore, (10) gives a relationship between the reaction order and the random walk exponent of the media where the reaction takes place. Note that for $f=1$, one has $X=2$ and (9) becomes the classical text book second-order reaction.

Let us recall the main approximations used, appart from both the two body relative diffusion concept [23] and the proportionality between N and t for multifractals, in order to derive the rate equations for fractal and multifractal media. Equation (6) is valid for a single random walker after a very large number of jumps. During the reaction, A particles diffuse as isolated random walkers that collide between them after a large number of jumps only for small values of the concentration. But if one starts with a certain initial coverage θ_0, then (even if θ_0 were small) the early stage of the reaction corresponds to collisions after small number of jumps, i.e. out of the range of validity of (6). Summing up, one expects that (9), which is based (6), would hold in the limit $\theta \to 0$ and for $\theta \ll \theta_0$.

For the sake of clarity in the presentation of the simulation results it is convenient to integrate (9); then for $\theta \to 0$ and $\theta \ll \theta_0$, one has

$$1/\theta^{1-X} \sim t \tag{11}$$

or equivalently:

$$\ln\theta \sim [1/(1-X)] \ln t. \tag{12}$$

Therefore, if the discussed arguments are valid a plot of $\ln\theta$ vs $\ln t$ would give a straight line and from its slope one should obtain the reaction order.

2.2. Temperature Programmed Reaction on Fractal Media

Turning our attention to temperature programmed desorption experiments, we note that the relationship between N and t can be written as

$$N \sim \int_{t_0}^{t} \exp(-E/kT)dt', \tag{13}$$

where the temperature could be an arbitrary function of the time. Defining a new time scale $t''(t)$ proportional to N in (12), and then replacing t by t'', all of (6, 8–10) hold. Therefore, in the time scale t the reaction rate (9) may be written as

$$-d\theta/dt = C'\theta^X \exp(-E/kT), \quad \theta \to 0 \text{ and } \theta \ll \theta_0, \tag{14}$$

where C' is a constant and X is given by (10). In order to compare (14) with the results of the simulations it is convenient to define

$$Y = -\exp(E/kT)d\theta/dt. \tag{15}$$

Therefore, one sees that a plot of $\ln Y$ vs $\ln\theta$ would give a straight line from whose slope the reaction order may be obtained.

3. *The Monte Carlo Procedure*

Due to the crude assumptions involved in obtaining (14) for temperature programmed reactions on fractal media and (9) for isothermal reactions on multifractal media with $X>2$ in both cases, the Monte Carlo simulation appears to be a suitable tool to check for the first time their validity. In fact, to our knowledge, (9) holds for one-dimensional chains and percolating clusters as demonstrated by means of computer simulations [22, 23] and also, for the last case, experimental results [23, 37]. Furthermore, the simulations allow us to investigate, for the first time to our knowledge, the recombination reaction within the whole coverage regime, in order to check the range of validity of the theoretical description.

These aims are also justified by the fact that thermal desorption spectroscopy is the most employed technique for the study of the absorbent-adsorbate interaction, see for example the reviews [38, 39]. It should also be mentioned that a recently developed measurement technique would provide useful information on thermal desorption data from large area fractal samples [40].

On the other hand, our aim is also to study the effect of chemisorbed impurities blocking active sites on the recombination reaction of A particles on percolating clusters, as a simple model for the poisoning of real fractal catalysts. In this case the Monte Carlo simulation is also useful since the theoretical arguments of Sect. 2 are not strictly valid, as will be discussed later.

For percolating clusters, the simulations have been carried out on square lattices of size $L=201$, randomly filled in at $p=0.593$. With these parameters the largest (percolating) cluster has $\cong 14{,}850$ particles in average. For the simulation of the reactions, only percolating clusters which have both their width and length equal to L are selected. After that, the cluster is covered with A particles at random with probability θ_0 (θ_0 is the initial coverage on the cluster). Double occupancy of cluster sites with A particles is forbidden.

Taking into account that most thermal desorption experiments are performed by uniformly raising the temperature of the sample, we have assumed a linear heating rate

$$T=T_0+\beta t, \tag{16}$$

where T_0 is the initial temperature, β is the heating rate, and in the simulation t is the Monte Carlo time step which is defined as proportional to the number of jumping attempts (i.e. the number of successful jumping events plus the failed ones) per particle (the proportionality constant used is 0.05).

After covering the cluster, the simulation of the reaction starts with the simultaneous heating of the sample. The jumping of an A particle to a nearest neighbour cluster site is determined at random by comparing the Boltzmann term $\exp[-E/kT]$, where E is the activation energy of diffusion (the same for all cluster sites), with a random number uniformly distributed between 0 and 1. Periodic boundary conditions for particle movement are assumed in order to avoid edge effects. The reaction described by (7) is considered successful when two A particles are at the same cluster site as a consequence of the jumps, then both particles are removed from the sample.

For the case of multifractal substrates, the simulations have been carried out on square lattices of size $L=256$, which corresponds to $n=8$ generations. The reaction between A particles is simulated as for percolating clusters, but the temperature remains constant through all the reaction and the jumping probabilities between adjacent sites are now given by (2).

4. Results

4.1. *Temperature Programmed Reactions on Percolating Clusters*

Figure 4 shows plots of $\ln Y$ vs $\ln\theta$ for temperature programmed reactions on percolation clusters at $p=0.593$ assuming $E=4$ kcal/mol, $\beta=1$ K/unit of Monte Carlo time. From the slopes of the straight lines [see (14, 15)] one obtains the reaction order $X=2.53$

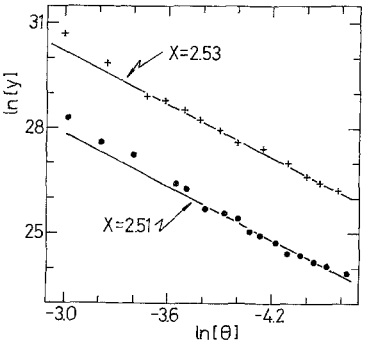

Fig. 4. Plot of $\ln Y$ vs $\ln\theta$, with $Y=-\exp(E/kT)\cdot d\theta/dT$ [see (14, 15)] for temperature programmed recombination reactions on percolating clusters. Lattice size $L=201$, $\beta=1$ K/unit of Monte Carlo time, $E=4$ kcal/mol. +, $\theta_0=0.10$ and ●, $\theta_0=0.20$, results averaged over 80 reactions. The slopes correspond to the asymptotic behaviour and have been evaluated by least-squares fits of the respective points for $\ln\theta\leqq -3.6$. The ordinate axis of the full circles has been shifted down by 2 units for the sake of clarity

for $\theta_0 = 0.10$ and $X = 2.51$ for $\theta_0 = 0.20$ within $0.01 \leqq \theta \leqq 0.05$. Similar plots have also been obtained for $\theta_0 \leqq 0.20$ and $0.1 \leqq \beta \leqq 10$ K/unit of Monte Carlo time, with slopes close to $X = 2.5$ for $0.01 \leqq \theta \leqq 0.05$. This result is in agreement with both the fact that replacing $f = 2/3$ for percolating clusters in two dimensions [25, 26] in (10) gives $X = 2.50$, and with previous Monte Carlo results for reactions at constant temperature [22, 23].

According to the theory of Sect. 2, and the results just discussed, (14) with $X > 2$ is valid for $\theta \ll \theta_0$ and $\theta \to 0$. Since the temperature programmed method allow us to investigate the behaviour of the reaction within the whole coverage regime, it is convenient to determine more precisely the range of validity of the theoretical predictions. From the results shown in Fig. 5 it follows that there are two well-defined regimes: the high coverage one ($0.4 \leqq \theta \leqq 1.0$), with the standard second order reaction behaviour ($X = 2$) and the medium-low coverage regime ($0 < \theta \leqq 0.4$) with an anomalous $X = 2.5$ reaction order. Let us stress the importance of this result because it suggests that the range of validity of the anomalous reaction rate equations is much wider than the expected one based on theoretical arguments. It is interesting to discuss whether the above statement could be influenced by the finite lattice size. With the parameters used in the simulation and the aid of (13) one can estimate the average number of jumps performed by a single random walker from the beginning of the reaction up to the low coverage regime where the reaction rate is negligible. For the example shown in Fig. 5 we obtain $N \sim 300$, so the average distance from the origin of the walker which is given by $R_N \sim \sqrt{N^{2\nu}}$ ($\nu = 0.352$ for the percolation cluster) is of the order of ~ 10, i.e. much

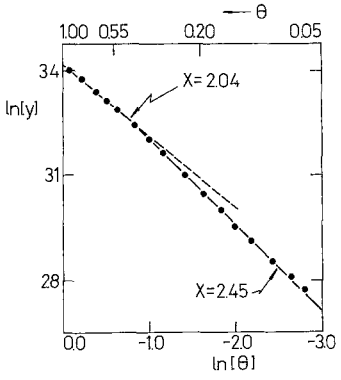

Fig. 5. Plot of $\ln Y$ vs $\ln\theta$, with $Y = -\exp(E/kT)d\theta/dt$ for the temperature programmed recombination reaction of particles on percolating clusters. Lattice size $L = 201$, $\beta = 10$ K/unit of Monte Carlo time, $E = 4$ kcal/mol and $\theta_0 = 1.0$. Results averaged over 120 reactions. The dashed line shows the slope of the high coverage regime ($0.4 \leqq \theta \leqq 1$, the coverage is indicated in the upper part of the figure). The full line corresponds to the slope obtained within the fractal (anomalous) regime

lower than the linear size of the lattice ($L = 201$). Therefore, we expect that the results are not influenced by artificial visitation due to finite size effects. The same statement holds for the results obtained working with multifractals (see Sect. 4.3).

Summing up, our results suggest that the reaction order of diffusion limited recombination reactions on fractal surfaces with $f < 1$ should be greater than the classical value $X = 2$. This conclusion, valid in the medium- and low-coverage regime, should affect intermediate steps of some complex reactions which take place in fractal (highly porous) catalysts.

4.2. The Influence of Chemisorbed Impurities Blocking Active Sites

The purpose of this subsection is to discuss the effect of chemisorbed impurities on the rate equation of the diffusion limited recombination of particles. It is assumed that each impurity atom blocks the site where it is chemisorbed i.e. the poison is represented by means of a hard-sphere exclusion model. Therefore, we are dealing with the purely geometric short range poisoning effect and the so-called electronic factor in heterogeneous catalysis, which arises due to the chemisorption of electronegative and/or electropositive atoms [41], is not considered.

The reaction is now simulated as follows: a percolating cluster is selected as indicated in Sect. 3. Then the poison is distributed at random on the cluster with probability δ_p (δ_p is the coverage of poison on the percolating cluster which remains constant throughout the produce). Also poisoned sites are not allow to diffuse. After that, the non-contaminated sites of the cluster are covered at random with A particles with probability θ_0. Then, the reaction is simulated as in Sect. 4.1, but now particle jumps into contaminated sites are forbidden.

Figure 6 shows a plot of $\ln Y$ vs $\ln\theta$ [see (14, 15)] for $L = 201$, $E = 4$ kcal/mol, $\beta = 1$ K/unit of Monte Carlo time and different values of δ_p. From the slopes of the obtained curves it follows that the reaction order increases with increasing δ_p. Since $X > 2$ and $\theta < 1$, (14) predicts that the rate of the reaction for the same values of E and T should decrease when increasing δ_p. This behaviour is evidenced in Fig. 7 where the coverage θ is plotted against the temperature. For the sake of comparison the evolution of θ vs T for a reaction on a homogeneous two-dimensional surface has also been included in Fig. 7. These results clearly show that the presence of geometrical heterogeneities causes the reaction to become slower compared to homogeneous surfaces, in the sense that, for the same temperature and initial conditions, θ is greater for percolating clusters than for the two-dimensional surface. Roughly

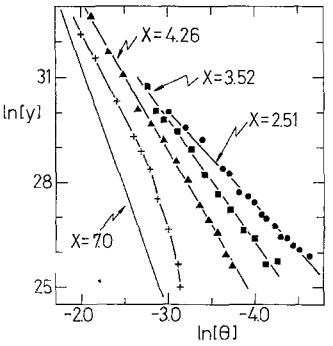

Fig. 6. Plot of $\ln Y$ vs $\ln\theta$, with $Y=-\exp(E/kT)d\theta/dt$ for temperature programmed recombination reactions on percolating clusters. Lattice size $L=201$, $\beta=1$ K/unit of Monte Carlo time, $E=4$ kcal/mol, and $\theta_0=0.20$, results averaged over 80 reactions. ●, $\delta_p=0$, results for poison-free percolating cluster shown for the sake of comparison. ■, $\delta_p=0.05$ and ▲, $\delta_p=0.10$. The corresponding slopes have been evaluated by the least-squares fit of all the points shown in the figure. +, $\delta_p=0.20$, in this case the point does not define the straight line and the reaction order increases when decreasing the coverage. A straight line with slope $X=7$ has been drawn for the sake of comparison

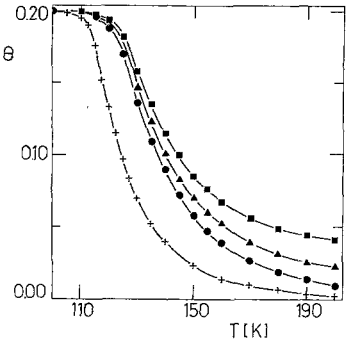

Fig. 7. The surface coverage θ vs T for temperature programmed recombination reactions. Lattice size $L=201$, $\beta=1$ K/unit of Monte Carlo time, $\theta_0=0.20$, $E=4$ kcal/mol. Results averaged over 80 reactions. +, homogeneous two-dimensional lattice with $\theta_p=0$. ●, poison-free percolating cluster ($\theta_p=1-p_c=0.407$, $\delta_p=0$). ▲, ■ contamined percolating clusters with $\delta_p=0.10$ and $\delta_p=0.20$, respectively

speaking, starting with the same initial coverage, one can also say that geometric poisoning of the percolating cluster at p_c causes a further decrease of the reaction rate. This is a delicate point which merits a further discussion.

In the thermodynamic limit ($L\to\infty$) and for arbitrary values of the probability in the percolation model ($0<p\leqq 1$) the number of different sites visited by the random walker on the largest cluster (6) may be written as:

$$S_N\sim t^{f_{\text{eff}}}, \tag{17}$$

where f_{eff} is an "effective" random walk exponent (for fractals $f_{\text{eff}}=\tilde{d}_{\text{eff}}/2$, where $\tilde{d}_{\text{eff}}$ is the effective spectral dimension $0<\tilde{d}_{\text{eff}}<2$ [42]). It is expected that

$$f_{\text{eff}}=\begin{cases}1 & \text{for } p>p_c\\ f=2/3 & \text{for } p=p_c\\ 0 & \text{for } p<p_c\end{cases}. \tag{18}$$

How can this behaviour of f_{eff} be related to our poisoning simulation experiments? Let us start with a poison-free infinite two-dimensional lattice. If we begin to deposite the poison randomly with probability θ_p, for $\theta_p<1-p_c\cong 0.41$, the largest poison-free site cluster is an infinite homogeneous percolation cluster and the reaction order with $f_{\text{eff}}=1$ becomes $X=2$, i.e. the classical result. (Note that θ_p is the poison concentration of the homogeneous two-dimensional substratum, while δ_p is the poison coverage of the percolating clusters.) At $\theta_p=1-p_c$, one has the infinite fractal percolation cluster of poison free lattice sites and $X=2.5$ [$f_{\text{eff}}=f=2/3$; see also (23)]. Finally, for $\theta_p>1-p_c$ there are only finite clusters of poison-free substratum particles. Then, the number of distinct sites visited by the walker becomes saturated at finite times, i.e. $f_{\text{eff}}=0$ for $t\to\infty$. Note that substituting $f_{\text{eff}}=0$ in (10) one has $X=\infty$, which would reflect the trivial case of many A particles, each of them on a different finite cluster, which cannot react, that is $d\theta/dt\sim\theta^X=0$ and as $0<\theta<1$ this means that $X=\infty$.

Considering the real simulations on finite lattices one expects that, starting from a poison-free substratum, the effect of the poison within the range $0\leqq\theta_p\leqq 1-p_c$ would be to cause a smooth change (instead of the abrupt one at $\theta_p=1-p_c$ in the $L=\infty$ limit) of the reaction order for the recombination of A particles from $X=2$ to $X=2.5$ for $t\to\infty$ ($\theta\to 0$). A further increase of θ_p causes the disaggregation of the poison-free percolating cluster into a certain number of non-percolating clusters, depending on δ_p. For this case and for $t\to\infty$ the same final result as for an infinite lattice, i.e. $X=\infty$ is expected. Nevertheless, this result has no practical interest and, additionally, the analytical tools discussed in Sect. 2 are only useful to predict the behaviour of the reaction for sufficiently small values of the concentration. On the other hand, the Monte Carlo method for finite reaction times on the disaggregated clusters remains as a practical alternative, which really shows that X increases for $\delta_p>0$. Note also that for $\delta_p=0.20$, the reaction order is not well defined in the sense that it depends on the surface coverage, as it is shown in Fig. 6.

Nevertheless, one should also mention that any relationship between δ_p and X for $\theta\to 0$ is only valid for the lattice size used in the respective simulation. In other words, one expects strong lattice-size effects in the dependence of X on δ_p and consequently experimental results with different sample sizes would give

different reaction orders (with $X>2.5$ for $\delta_p>0$ or $X>2$ for $\theta_p>0$). On the other hand, for large values of δ_p, it is also expected that the structure of the finite clusters (branched or compact) would be irrelevant for the reaction order, provided that the clusters are small enough.

4.3. *Isothermal Reactions on Multifractal Substrata*

Figure 8 shows plots of $\ln\theta$ vs $\ln t$ for the isothermal recombination of A particles on multifractal substrate. The long time behaviour of the simulation results shown in Fig. 8 gives straight lines in agreement with the theoretical predictions [see (12)]. The data obtained for f from the slopes of these lines and by using (12) and (10) are summarized and compared with the results previously published by Meakin [31] for simple random walkers on the same type of substrate, in Table 1. Note that the results obtained with the simulated reaction between walkers are in remarkably good agreement with those previously obtained [31] for isolated walkers. In this sense, we conclude that the simulation of the recombination reaction is a suitable alternative method for the determination of the random walk exponent, which has the advantage that the result of a single reaction simulation involves an average of many random walkers placed at different sites which cover all the substratum. Furthermore, the reaction order can easily be determined experimentally, unlike the random walk exponent which, however, plays an important role in many theoretical studies.

The results of the simulations on substrate with multifractal distribution of site probabilities, also

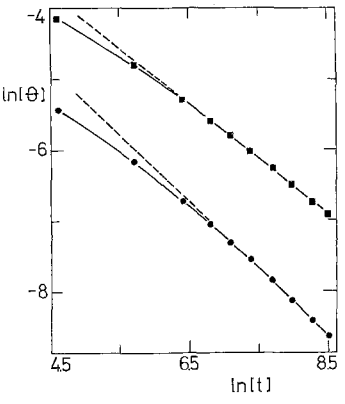

Fig. 8. Plot of $\ln\theta$ vs $\ln t$ [see (12)] for isothermal recombination reactions on multifractal substrata. $L=256$, $\theta_0=0.20$ and the probabilities of the multifractal are $P_m=CR^{m-1}$; $m=1,\ldots,4$ [see (6, 5)], with ■, $R=3/4$ and ●, $R=1/2$. The dashed straight lines show the long time behaviour and their slopes are employed to determine the reaction order listed in Table 1. For $R=1/2$ the ordinate axis has been shifted for the sake of clarity. Results are averaged over 80 reactions

Table 1. Exponents obtained for walkers in multifractals with $P_m=CR^{m-1}$; $m=1,\ldots,4$ [see (4, 5)]. X is the reaction order for the recombination of walkers obtained from the slopes of curves such as those shown in Fig. 8, with an error bar of about $\pm 10\%$. The lattice size used is $L=256$. f is the random walk exponent obtained inserting the respective value of X in (10). ξ and ξ' are the random walk exponents obtained by Meakin [31] for single random walkers, assuming $S_N\sim N^{\xi}$ and $S_N\sim[N/\ln N]^{\xi'}$, respectively; and on square lattices of size $L=1024$

R	X	f	ξ	ξ'
3/4	2.04	0.96	0.885	0.985
1/2	2.27	0.79	0.769	0.856
1/4	2.79	0.56	0.541	0.603

suggest that the reaction order of diffusion limited recombination reactions increases due to the presence of energetic heterogeneities on the surface. Therefore, the reaction rate at the low concentration regime of these reactions becomes slower than the rate classically expected on isoenergetic surfaces.

5. Conclusions

We have performed Monte Carlo simulations of the diffusion limited recombination reactions of particles on multifractal substrata and temperature programmed reactions of the same type, on percolating clusters with and without poisoned sites. From the results obtained, valid in the low coverage regime, we conclude that:

1) The reaction order for the thermal desorption of recombining particles on two-dimensional percolating clusters at p_c is $X=2.5$. As $f=2/3$, this result is in agreement with (10).

2) The reaction orders for recombination reactions at constant temperature on two-dimensional multifractal lattices characterized by the parameter R (for $R=3/4$, 1/2, and 1/4) are in agreement with (10) using the available values of f.

3) From conclusions 1) and 2) we expect (10) to hold for both temperature programmed reactions on geometrically heterogeneous fractals with isoenergetic sites and for reactions at constant temperature on energetically heterogeneous multifractals, in general.

4) On the light of conclusion 3), the experimental determination of the reaction order would allow us to calculate the random walk exponent of the corresponding fractal or multifractal media.

5) The presence of impurities (poison) blocking active sites of the percolation clusters would cause an additional increase of the reaction order. Finite sample size effects make difficult the assignment of an un-

equivocal relationship between the reaction order and the concentration of poison, but the above mentioned trend is beyond any doubt.

Concerning the range of validity of the fractal chemical kinetic equations, it should be mentioned that, from the theoretical point of view, it is expected that (10) only holds for $\theta \to 0$ and $\theta \ll \theta_0$. Nevertheless, our simulation results for the thermal desorption of recombining particles on two-dimensional percolating clusters at $p = 0.593$ show that $X = 2.5$ [i.e. fractal behaviour in agreement with (10)] for the medium and low coverage regime (i.e. $\theta \leqq 0.4$). In fact at $\theta \cong 0.4$ one has a crossover between the classical and the fractal behaviour.

We hope that our simulation results will stimulate careful experiments of recombination reactions on rough samples in order to check the validity of the theoretical conclusions.

References

1. B.B. Mandelbrot: *The Fractal Geometry of Nature* (Freeman, San Francisco 1982)
2. Proc. Sixth Trieste Int. Symp. on Fractal Physics, ed. by L. Pietronero, E. Tosatti (North-Holland, Amsterdam 1986)
3. *On Growth and Form*, ed. by H.E. Stanley, N. Ostrowsky (M. Nijhoff, Dordrecht 1986)
4. D. Stauffer: Phys. Rev. **54**, 1 (1979)
5. H.J. Herrmann: Phys. Rep. **136**, 153 (1986)
6. D. Stauffer, A. Coniglio, M. Adam: Adv. Polym. Sci. **44**, 103 (1982)
7. P. Pfeifer, D. Avnir, D. Farin: Surf. Sci. **126**, 569 (1983)
8. P. Pfeifer: Appl. Surf. Sci. **18**, 146 (1984)
9. P. Pfeifer, D. Avnir, D. Farin: J. Stat. Phys. **36**, 699 (1984); **33**, 263 (1985)
10. D. Avnir, D. Farin, P. Pfeifer: Nature **308**, 261 (1984)
11. D. Farin, D. Avnir: J. Am. Chem. Soc. (preprint)
12. D. Avnir: Materials Res. Soc. Symp. Proc. **73**, 231 (1986), ed. by C.J. Brinker
13. D. Romeu, A. Gómez, J.G. Perez-Ramirez, R. Silva, O.L. López, A.E. González, M.J. Yacaman: Phys. Rev. Lett. **57**, 2552 (1986)
14. H. van Damme, P. Levitz, F. Bergaya, J.F. Alcozer, L. Gatineau, J.J. Fripiat: J. Chem. Phys. **85**, 616 (1986)
15. J.E. Martin, A.J. Hurd: J. Appl. Cryst. **20**, 61 (1987)
16. S.H. Ng, C. Fairbridge, B.H. Kaye: Langmuir **3**, 340 (1987)
17. A. Kapitulnik, G. Deutscher: Phys. Rev. Lett. **49**, 1444 (1982); J. Stat. Phys. **36**, 815 (1984)
18. R.F. Voss, R.B. Laibowitz, E.I. Allesandrini: Phys. Rev. Lett. **43**, 1441 (1982)
19. D.A. Weitz, J.S. Huang, M.Y. Lin, J. Sung: Phys. Rev. Lett. **53**, 1657 (1984)
20. M. Matsushita, M. Sano, Y. Hayakawa, H. Honjo, Y. Sawada: Phys. Rev. Lett. **53**, 286 (1984)
21. L.W. Anacker, R. Kopelman, J.S. Newhouse: J. Stat. Phys. **36**, 591 (1984)
22. J.S. Newhouse, R. Kopelman: Phys. Rev. B **31**, 1677 (1985)
23. R. Kopelman: J. Stat. Phys. **42**, 185 (1986)
24. A. Takani, N. Mataga: J. Phys. Chem. **91**, 618 (1987)
25. S. Alexander, R. Orbach: J. Physique Lett. **43**, L625 (1982)
26. R. Rammal, G. Toulouse: J. Physique Lett. **44**, L13 (1983)
27. D.C. Rapaport: J. Phys. A **18**, L175 (1985)
    B. Derrida, D. Stauffer: J. Physique **46**, 1623 (1985)
28. E.V. Albano, H.O. Mártin: Thin Solid Films **151**, 121 (1987)
29. A. Kapitulnik, A. Aharony, G. Deutscher, D. Stauffer: J. Phys. A **16**, L269 (1983)
30. A. Coniglio: Physica **140**A, 51 (1986)
31. P. Meakin: J. Phys. A **20**, L771 (1987)
32. H.G.E. Hentschel, I. Procaccia: Physica **8**D, 435 (1983)
33. T.C. Halsley, M.H. Jensen, L.P. Kadanoff, I. Procaccia, B.I. Shraiman: Phys. Rev. A **33**, 1141
34. R. Benzi, G. Paladin, G. Parisi, A. Vulpiani: J. Phys. A **17**, 3521 (1984)
35. N. Metropolis, A.W. Rosenbluth, M.N. Rosenbluth, A.H. Teller, E. Teller: J. Chem. Phys. **21**, 1087 (1953)
36. L.W. Anacker, R. Kopelman: J. Chem. Phys. **81**, 6402 (1984)
37. P.W. Klynko, R. Kopelman: J. Phys. Chem. **87**, 4565 (1983)
38. G. Comsa, R. David: Surface Sci. Rep. **5**, 145 (1985)
39. A. King: Surface Sci. **47**, 384 (1975)
40. P. Basu, J. Yates, Jr.: Surf. Sci. **177**, 291 (1986)
41. J.K. Norskov, S. Halloway, N.D. Lang: Surf. Sci. **137**, 65 (1984)
42. P. Argyrakis, R. Kopelman: J. Chem. Phys. **81**, 1015 (1984)